

Short Communication

Reaction Mechanism Characterization of $\text{La}_{0.5}\text{Sr}_{0.5}\text{CoO}_{2.91}$ Electrocatalyst for Rechargeable Li-air Battery

Changwei Shi, Jiangang Feng, Lei Huang, Xue Liu, Liqiang Mai*

State Key Laboratory of Advanced Technology for Materials Synthesis and Processing, WUT-Harvard Joint Nano Key Laboratory, Wuhan University of Technology, Wuhan, 430070 P.R. China

*E-mail: mlq518@whut.edu.cn

Received: 20 May 2013 / Accepted: 15 June 2013 / Published: 1 July 2013

Li-air batteries have ultra-high capacity and energy density, however, the reaction mechanism is unclear because of the limits on characterization method. To further investigate the reaction mechanism of Li-air battery based on hierarchical mesoporous perovskite $\text{La}_{0.5}\text{Sr}_{0.5}\text{CoO}_{2.91}$ nanowires electrocatalyst which constructed in our previous work, we investigate the discharge reaction product by in-situ transmission electron microscope (TEM) and Raman spectrum. The increase of carbon/oxygen ratio value after electron beam irradiation and the lattice vibration are observed thus demonstrating the existence of Li_2O_2 . Further Raman spectrum investigation indicates that some impurities insert into the carbon. Besides, a possible catalytic mechanism was proposed by analyzing ligand field.

Keywords: electrocatalysis, Li-air battery, mechanism characterization, in-situ TEM

1. INTRODUCTION

Lithium-air batteries are regarded as next generation energy storage device due to their highest energy density among the chemical batteries. However, some challenges exist in Li-air battery research. [1-7] Firstly, the fast capacity decay happens with the increase of cycles because the products of discharge reaction can accumulate and further blocking the oxygen pathway. [8, 9] Secondly, the reaction mechanism is uncertain. [1] Recent study has demonstrated that reactions at the O_2 cathode are dominated by reversible Li_2O_2 formation/decomposition. [10] However, the degradation of electrolyte especially based on organic carbonates (for example, LiPF_6 in propylene carbonate) does indeed occur on discharge. [8] The products of electrolyte decomposition accumulate with the increase on cycling, which induce the difficulty of characterizing Li_2O_2 formation occurring in parallel with the degradation. Confined by analytical tools, Fourier transform infrared, Raman and mass spectrometry have been

used to demonstrate the formation of Li_2O_2 on discharge process,[8, 10, 11] which is not enough for the conviction.

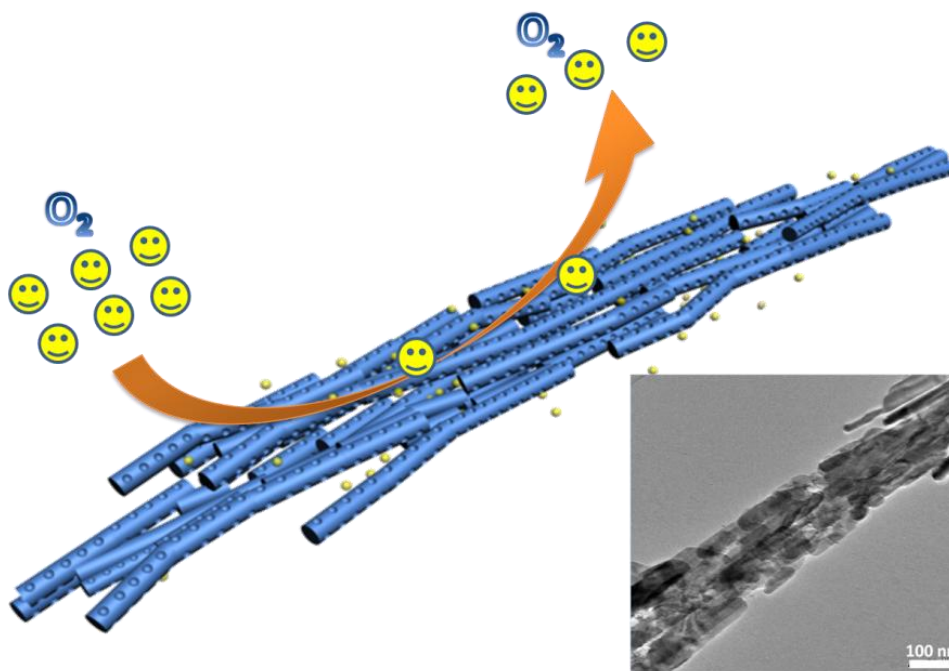


Figure 1. The scheme of hierarchical mesoporous perovskite LSCO nanowires structure, inset is TEM image of nanowires.

For the first challenge, in our recent work, we have synthesized hierarchical mesoporous perovskite $\text{La}_{0.5}\text{Sr}_{0.5}\text{CoO}_{2.91}$ (LSCO) nanowires with tri-continuous tunnels for oxygen transport, ion diffusion and electron conduction (Figure 1).[12] Intrinsic oxygen reduction reaction (ORR) and oxygen evolution reaction (OER) testing via rotating disk electrode (RDE) indicating that it is a kind of high-performance catalyst for the ORR and OER with low peak-up potential and high limiting diffusion current. However, the reaction mechanism characterization did not be considered in our previous work because the accumulation of electrolyte decomposition products leads to the difficulty of characterization of Li_2O_2 .

To achieve reversible cycling and impede the electrolyte decomposition in $\text{Li}-\text{O}_2$ system, we extended the battery test by limiting specific capacity. In this work, the hierarchical mesoporous perovskite $\text{La}_{0.5}\text{Sr}_{0.5}\text{CoO}_{2.91}$ nanowires electrocatalyst acts as electrocatalyst and the 25 charge/discharge cycles with stable specific capacity of 1000 mAh g^{-1} can be achieved. The product of discharge reaction was characterized by in-situ HRTEM and Raman spectrum after first discharge. The Li_2O_2 is observed through the increase of carbon/oxygen value and lattice fringe image of lithium metal after electron beam irradiation under the HRTEM. The Raman spectrum after discharge comparing with pristine carbon further confirmed the discharge products insert into the active carbon. Additionally, a catalytic mechanism was proposed based on ligand field theory.

2. EXPERIMENTAL

The synthesis of hierarchical mesoporous perovskite $\text{La}_{0.5}\text{Sr}_{0.5}\text{CoO}_{2.91}$ (LSCO) nanowires through multi-step micro-emulsion self-assembly method followed by annealing is described in our previous paper.[12]

0.75 mg hierarchical mesoporous LSCO nanowires mixed with 4.25 mg AC and 122 μL of 5wt% Nafion solutions were dispersed in 1 mL of 3:1 vol/vol water/isopropanol mixed solvent by at least 30 min sonication to form a homogeneous ink. 2 mg of sample from ink was loaded on a piece of filter paper. The electrochemical properties were carried out by assembling 2032 coin cells in a glove box filled with pure oxygen gas, using a lithium pellet as the anode, and filter paper-supported samples as cathode. Galvanostatic discharge was studied with limited specific capacity of 1000 mAh g^{-1} in a potential range of 4.2-2.0 V vs. Li/Li⁺ with a multichannel battery testing system (LAND CT 2001A).

After first discharge, the battery was disassembled and ultrasonic cleaning treatment was taken to remove electrolyte. Then, the transmission electron microscopy (TEM), high-resolution transmission electron microscopy (HRTEM) was recorded by using a JEOL JEM-2010 FEF microscope at an accelerating voltage of 200 kV. Energy dispersive spectroscopy (EDS) was performed on a JEM 2100F STEM/EDS and the X-ray energy resolution is 132 eV. Laser Raman Spectrometer was recorded using the INVIA, Renishaw.

3. RESULTS AND DISCUSSION

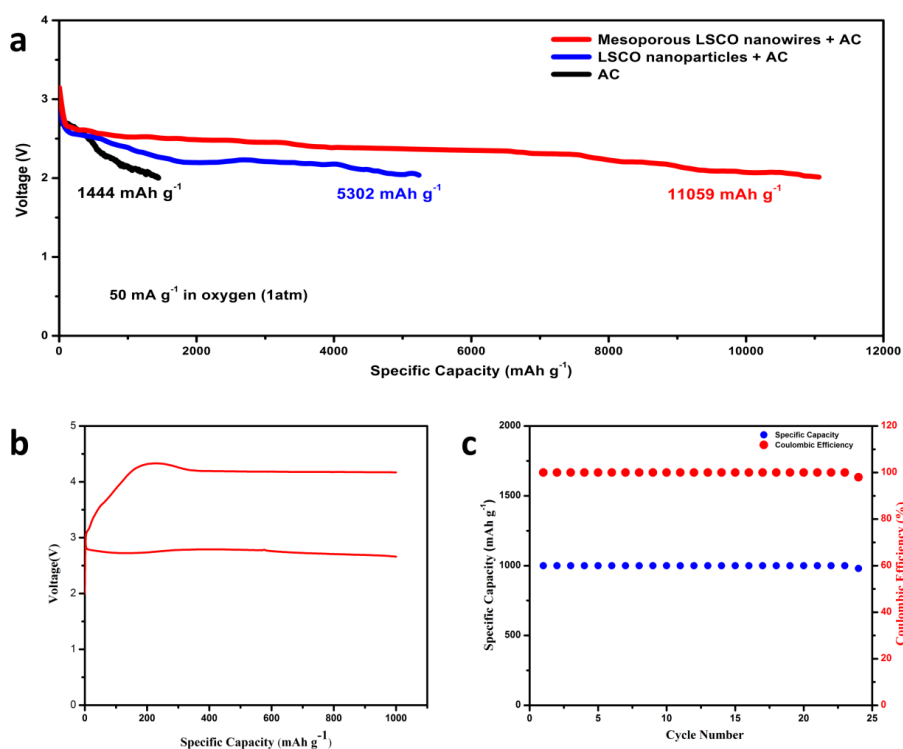


Figure 2. (a) The discharge curve of Li-air batteries. Copyright 2012, Proceedings of the National Academy of Sciences. (b, c) Electrochemical performance of Li-air batteries with the limited capacity of 1000 mAh g^{-1} . (b) Charge/discharge curve, (c) cycling performance.

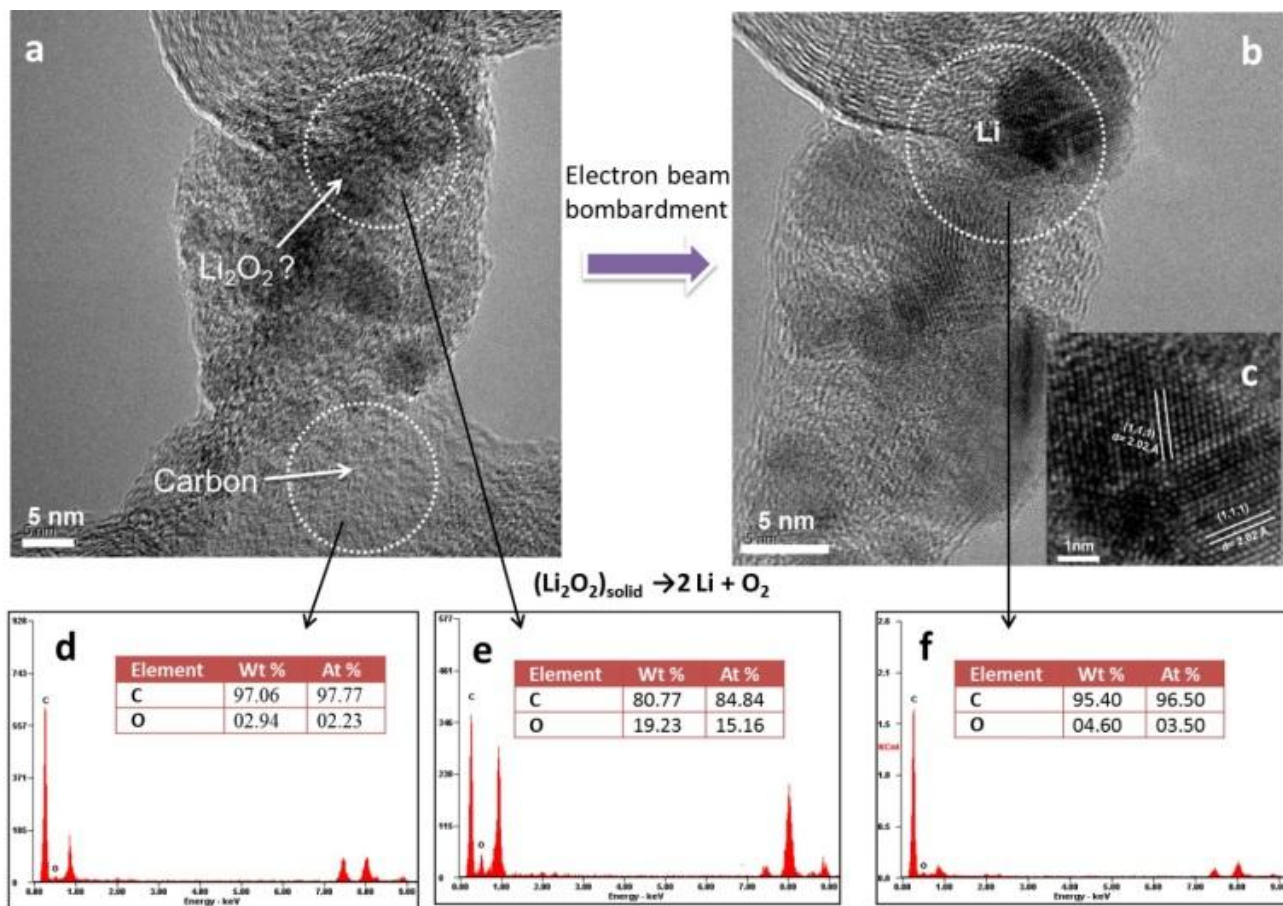


Figure 3. (a, b) TEM image of activated carbon before and after electron beam bombardment. (c) HRTEM of crystal on selected areas. (d, e, f) The EDS microanalysis on selected areas.

In previous work of organic carbonate electrolyte Li-air batteries, the ultra-high first discharge capacity can be achieved, especially for hierarchical mesoporous LSCO nanowires cathode (Figure 2a). However, the fast fading happens in following cycles because the products of electrolyte decomposition accumulate on the electrode surface, further inducing the increase of resistance, the decline of catalytic active site and the block of oxygen transport pathway. In this work, the specific capacity can maintain 1000 mAh g⁻¹ in 25 cycles with no capacity fading while current density at 0.1 A g⁻¹ (Figure 2c). Figure 2b shows the discharge plateau at the voltage of ~2.8 V, thus indicating the adverse reactions can be well restrained with limited capacity. [13-15] It well demonstrates that the electrolyte is stable at this situation. The stability of electrolyte benefits to avoid the by-product formation and helps the detection of Li₂O₂.

After disassembling battery and ultrasonic cleaning treatment, the TEM characterization is performed to investigate the reaction product. Under HRTEM, Lattice fringes of LSCO will cover up Li₂O₂, thus amorphous carbon is selected as standard. In Figure 2a, low crystallinity lattice fringes were observed in the amorphous carbon. The EDS microanalysis on selected areas are shown in Figure 2d, e, and only C and O exist (Li is undetected). From amorphous area to lattice fringes area, O increase from 3.94 wt% to 19.23 wt%, which suggested there may be lithium oxides. And from HRTEM video (Supplementary information), lattice vibration was obtained only in the lattice fringes

area, which indicates the structure is unsteady. Surprisingly, crystallinity increased after electron beam irradiation (Fig. 3b). In addition, the lattice fringes with interplanar distances of 2.02 Å are characteristic of Li metal in the (111) plane (Figure 3c) indicating the formation of Li metal under HRTEM. The secondly-EDS on selected areas show that the O was decreased to 4.6 wt%.

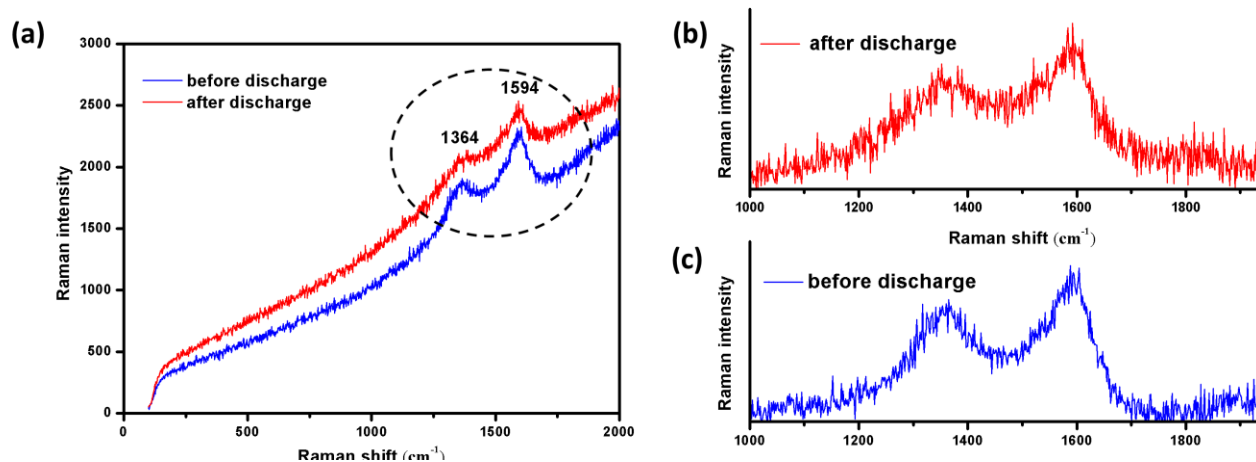


Figure 4. (a) Raman spectrum of electrode before and after discharge. (b, c) Zoom-in images captured from oval region of (a).

Those studies suggest the reaction $(\text{Li}_2\text{O}_2)_{\text{solid}} \rightarrow 2 \text{Li} + \text{O}_2(1)$ did take place. Combining the results from EDS and TEM, it demonstrates that Li_2O_2 is main product of Li-air battery reaction. Meanwhile, Raman spectroscopy was applied to investigate the change on active carbon. As figure 4 shows, the peak at 1364 and 1594 cm^{-1} corresponding to D and G modes of carbon are both detected before and after discharge.[16] However, the Raman peaks broaden after discharge, indicating some impurities (i.e. Li_2O_2) insert into the carbon. Therefore, conclusions from Raman analysis are similar to them from HRTEM.

Based on the above results, a possible catalytic mechanism was proposed by analyzing ligand field. [17] As we know, the chemisorption of reactants has great possibility to be rate control process during catalytic process. [18-20] During electrocatalytic process of oxygen, the dissociative oxygen (O_{dis}) firstly is chemisorbed by $\text{Co}^{3+}/\text{Co}^{4+}$ and forms adsorbed oxygen (O_{ads}) followed by an electron injection process (generalized as: $\text{O}_2 + e^- \rightarrow \text{O}_2^-$). In this case, the kinetics sluggish of oxygen chemisorption could occur since it has been demonstrated in most non-noble metals catalytic systems. [6,21]

We proposed coordination of cobalt and O_{dis} can be strengthened through σ - π bonding. Firstly, the d orbit of Co^{II} firstly can be split into e_g and t_{2g} in the asymmetric disturbed field. [22] The electron in d band of Co^{II} prefer to filling the e_g orbit because the oxygen molecular is a kind of weak field ligand. [23] The e_g electron tends to bind with oxygen's σ^*2p electron to form σ bond. Furthermore, the t_{2g} electron can interact with π^*2p electron of O_{dis} . Consequently, the O_{ads} has forceful enough coordination with cobalt and enables the efficiency of next-step electron injection.

4. CONCLUSION

In summary, more stable Li-air battery system can be realized by limiting the charge/discharge capacity. Good cycling performance with low degree of electrolyte decomposition can be achieved. Formation of Li_2O_2 is confirmed through in-situ TEM and Raman spectrum thus demonstrating the reaction mechanism of Li-air battery. Additionally, the catalytic mechanism was proposed by analyzing ligand field. The reaction mechanism research is benefit to optimizing the electrocatalyst design and constructing better Li-air batteries.

ACKNOWLEDGEMENTS

This work was supported by the National Basic Research Program of China (2013CB934103, 2012CB933003), the National Natural Science Foundation of China (51072153, 51272197), the Program for New Century Excellent Talents in University (NCET-10-0661), and the Fundamental Research Funds for the Central Universities (2012-II-001, 2013-YB-001). Thanks to Professor CM Lieber of Harvard University, Professor DY Zhao of the Fudan University, Professor J Liu of the Pacific Northwest National Laboratory, and Professor ZL Wang of Georgia Institute of Technology for their strong support and stimulating discussions.

References

1. M. Armand, J. M. Tarascon, *Nature*, 451 (2008) 652.
2. B. Dunn, H. Kamath, J. M. Tarascon, *Science*, 334 (2011) 928.
3. P. G. Bruce, S. A. Freunberger, L. J. Hardwick, J. M. Tarascon, *Nat. Mater.*, 11(2011)19.
4. Y. C. Lu, Z. Xu, H. A. Gasteiger, S. Chen, K. Hamad-Schifferli, Y. Shao-Horn, *J. Am. Chem. Soc.*, 132 (2010) 12170.
5. Y. Cui, Z. Wen, Y. Liu, *Energ. Environ. Sci.*, 4 (2011) 4727.
6. J. Suntivich, H. A. Gasteiger, N. Yabuuchi, H. Nakanishi, J. B. Goodenough, Y. Shao-Horn, *Nat. Chem.*, 3(2011) 546.
7. H. G. Jung, J. Hassoun, J. B. Park, Y. K. Sun, B. Scrosati, *Nat. Chem.*, 4 (2012) 579.
8. [8] S. A. Freunberger, Y. Chen, Z. Peng, J. M. Griffin, L. J. Hardwick, F. Bardé, P. Novák, P. G. Bruce, *J. Am. Chem. Soc.*, 133 (2011) 8040.
9. J. Xiao, D. Wang, W. Xu, D. Wang, R. E. Williford, J. Liu, J. G. Zhang, *J. Electrochem. Soc.*, 157(2010) A487.
10. Y. Chen, S. A. Freunberger, Z. Peng, F. Bardé, P. G. Bruce, *J. Am. Chem. Soc.*, 134 (2012) 7952.
11. S. A. Freunberger, Y. Chen, N. E. Drewett, L. J. Hardwick, F. Bardé, P. G. Bruce, *Angew. Chem. Int. Edit.*, 50 (2011) 8609.
12. Y. Zhao, L. Xu, L. Mai, C. Han, Q. An, X. Xu, X. Liu, Q. Zhang, *P. Natl. Acad. Sci. USA.*, 109 (2012) 19569.
13. Z. Peng, S. A. Freunberger, Y. Chen, P. G. Bruce, *Science*, 337 (2012) 563.
14. Y. C. Lu, B. M. Gallant, D. G. Kwabi, J. R. Harding, R. R. Mitchell, M. S. Whittingham, Y. Shao-Horn, *Energ. Environ. Sci.*, 6 (2013) 750.
15. T. Zhang, H. Zhou, *Nat. Comm.*, 4 (2013) 1817.
16. L. M. Malard, M. A. Pimenta, G. Dresselhaus, M. S. Dresselhaus, *Phys. Rep.*, 473(2009) 51.
17. B. N. Figgis, *Trans. Faraday Soc.*, 57 (1961) 198.
18. N. Russo, D. Mescia, D. Fino, G. Saracco, V. Specchia, *Ind. Eng. Chem. Res.*, 46 (2007) 4226.
19. L. Zhang, Z. Xia, *J. Phys. Chem. C*, 115 (2011) 11170.

20. E. J. Crumlin, E. Mutoro, S. Ahn, G. J. la O', D. N. Leonard, A. Borisevich, M. D. Biegalski, H. M. Christen, Y. Shao-Horn, *J. Phys. Chem. Lett.*, 1 (2010) 3149.
21. M. Kumar, R. Awasthi, A.K. Pramanick, R.N. Singh, *Int.J.Hydrogen Energ.*, 36 (2011) 12698.
22. J. L. Hueso, J. P. Holgado, R. Pereñíguez, S. Mun, M. Salmeron, A. Caballero, *J. Solid State Chem.*, 183 (2010) 27.
23. M. Nakamura, *Angew. Chem. Int. Edit.*, 48 (15) 2638.